福昕PDF编辑器

• 永久　• 轻巧　• 自由

升级会员　　批量购买

永久使用

无限制使用次数

极速轻巧

超低资源占用，告别卡顿慢

自由编辑

享受Word一样的编辑自由

扫一扫，关注公众号

A Local Contrast Method for Infrared Small-Target Detection Utilizing a Tri-Layer Window

Jinhui Han, Saed Moradi, Iman Faramarzi, Chengyin Liu, Honghui Zhang, and Qian Zhao

***Abstract*— Local contrast has been proved efficient for infrared (IR) small-target detection. However, current algorithms do not enhance true target purposefully before local contrast calculation and may easily be disturbed by noises. In this letter, a new detection framework named multiscale tri-layer local contrast measure (TLLCM) is proposed. First, a tri-layer filtering window is proposed, and it consists of a core layer, a reserve layer, and a surrounding layer. The idea of a matched filter is adopted, and a Gaussian filtering will be performed on the core layer to enhance true target purposefully according to the target shape. Then, the multiscale TLLCM of the central pixel of the window will be calculated between the enhanced core and the surrounding local background. Finally, the target can be extracted by an adaptive threshold. Experimental results show that the proposed method can achieve better detection performance than some existing algorithms.**

***Index Terms*— Infrared (IR) small target, local contrast, matched filter, multiscale detection, tri-layer window.**

I. Introduction

INFRARED search and track (IRST) systems have been widely used in the fields of precise guidance, prewarning, remote sensing, and so on [1]. However, if a target is far from the detector, it will occupy only a few pixels without obvious shape or texture in the acquired image, which is usually referred as IR small target [2]. The detection of IR small target is usually very difficult because the target is only a dim and small spot [3], and it can be easily drowned by complex backgrounds. Meanwhile, there are usually some bright background [4] or targetlike interferences (such as broken clouds [5] and pixel-sized noises with high brightness (PNHB) [6], etc.) in the image, and they may easily be mistaken as targets.

In recent years, the local contrast mechanism of the human visual system has been introduced in the field of IR small target detection. For example, Kim *et al.* [7] proposed a filter template named Laplacian of Gaussian (LoG), Wang *et al.* [8] proposed a similar template named difference of Gaussian (DoG), and they can effectively enhance true target and suppress flat background. However, they are sensitive to background edges. To suppress background edges better, Shao *et al.* [9] combined LoG with morphological method; Han *et al.* [10] replaced the Gaussian kernel with Gabor kernel; Wang *et al.* [11] combined DoG with frequency-domain method; Nasiri *et al.* [12] proposed a tri-layer template; and so on.

After further analysis, researchers found that a true target usually appears as a circular compact spot attenuating roughly evenly from center to boundary due to the point spread function of the optical system, and background edges usually distribute along a specific direction at local [13]. Therefore, some researchers tried to suppress background edges using directional information. For example, Chen *et al.* [14] proposed the local contrast measure (LCM), and it used a nested structure with eight directions; Han *et al.* [6] used an average operation to suppress PNHB; Qin and Li [15] indicated that only some maximal pixels should be considered during averaging; Wei *et al.* [16] merged two corresponding directions together; Han *et al.* [17] proposed a relative local contrast method; Nie *et al.* [18] considered the local homogeneity; and so on. In addition, many joint algorithms had been proposed. For example, Deng *et al.* [19] used entropy as a weighting function for local contrast; Cui *et al.* [20] combined local contrast with compressed sensing; Moradi *et al.* [21] combined local contrast with Laplacian of point spread function; Xia *et al.* [22] combined local contrast with modified random walks; Han *et al.* [23] combined local contrast with adaptive background estimation; and so on.

Generally, LCM and its improvements take the directional information into account and can suppress background edges better; however, there are still some problems regarding these algorithms. First, the contrast information is usually directly calculated between the original value of the central cell and the surrounding cells of a nested structure, but when the target is dim, the distinction between them will not be obvious. Second, current algorithms do not fully consider the shape of true target and enhance it purposefully, so they may be easily disturbed by noises.

In this letter, a new detection framework named multiscale tri-layer LCM (TLLCM) is proposed. Before calculating the local contrast, the target will be enhanced first to make the distinction between the target and the background obvious enough. In the processing of the target enhancement, the central cell of the nested structure is divided into the core layer and the reserve layer. The idea of the matched filter is adopted and a Gaussian template will be applied on the core layer to

Manuscript received May 28, 2019; revised August 6, 2019; accepted September 4, 2019. This work was supported in part by the National Natural Science Foundation of China under Grant 61802455 and Grant 11847113, in part by the Foundation of the Education Department of Henan Province under Grant 18B510021, and in part by the Foundation of the Science and Technology Department of Henan Province under Grant 182102410065 and Grant 192102210089. *(Corresponding author: Jinhui Han.)*

J. Han, H. Zhang, and Q. Zhao are with the College of Physics and Telecommunication Engineering, Zhoukou Normal University, Zhoukou 466001, China (e-mail: hanjinhui@zknu.edu.cn).

S. Moradi is with the Department of Electrical Engineering, University of Isfahan, Isfahan 817746-73441, Iran.

I. Faramarzi is with the Faculty of Electrical and Computer Engineering, Malek-e-Ashtar University of Technology, Tehran 158751774, Iran.

C. Liu is with the Wuhan Electronic Information Institute, Wuhan 430074, China.

Color versions of one or more of the figures in this letter are available online at http://ieeexplore.ieee.org.

Digital Object Identifier 10.1109/LGRS.2019.2954578

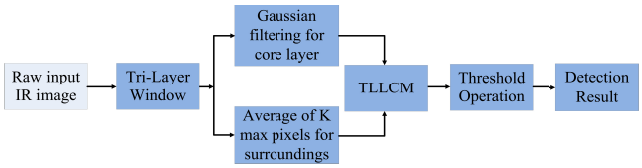

Fig. 1. Flowchart of the proposed TLLCM algorithm.

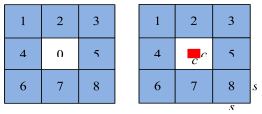

Fig. 2. (Left) Double-layer window used in current algorithms. (Right) Tri-layer window used in the proposed algorithm.

enhance target purposefully. The contrast information will be calculated between the enhanced target and the surrounding background, and the true target can be extracted by a simple adaptive threshold operation.

II. Proposed Algorithm

The flowchart of the proposed algorithm is shown in Fig. 1. First, a tri-layer filtering window is proposed, in which the core layer is used to capture the main energy of a target, the reserve layer is used to separate the target from its neighboring, and the surrounding layer is used to capture the surrounding background of the target. Then, the idea of matched filter is introduced and a Gaussian filtering operation is performed on the core layer to enhance true target purposefully, and the average of the K maximal pixels is calculated for each surrounding cell to suppress background. Then, the multiscale TLLCM of the central pixel of the window will be calculated between the enhanced core and the surrounding local background. Finally, after all the pixels are calculated, a simple threshold operation will be used to extract the target.

A. Construction of the Tri-Layer Filtering Window

Current algorithms, for example, LCM and its improvements, usually use a double-layer nested window, in which the central cell is used to capture the whole target, and the surrounding cells are used to capture the background, see Fig. 2 (left). The local contrast information will be directly calculated between the central cell and the surrounding cells.

In this letter, we propose a new framework, in which the target will be enhanced first before the calculation by using a Gaussian filter (see Section II-B). However, as well known, the Gaussian filter can blur the image, and the larger the filter template, the more obvious the burring effect. It is well known that according to SPIE, a small target usually has a total spatial extent of less than 80 pixels [14], ranging from 2×2 to about 9×9 pixels [24]. To capture the whole target, the maximum central cell should also be set to at least 9×9. If we directly perform the Gaussian filter on the whole central cell, the image quality will degrade significantly. Thus, we decide to divide the central cell into two parts, i.e., the core layer and the reserve layer, see Fig. 2 (right). The core layer is used to capture the main energy of a target near its center, on which the Gaussian filter will be applied, and its size $c \times c$ is fixed to 3×3, so as to minimize the blurring effect. The reserve layer is used to separate the target from its neighboring, and its size $s \times s$ (also equal to the size of each surrounding cell) will be adjusted according to the target size. If the target size is unknown, multiscale detection will be needed.

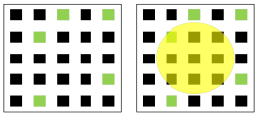

Fig. 3. Different cases when noises exist in the central cell. (Left) All the noise pixels (green dots) will be considered when $K > 5$ for NLCM and RLCM. (Right) Only one noise pixel will be considered since a Gaussian filter template (yellow circle) is adopted in the proposed algorithm.

B. Multiscale TLLCM Calculation

Applying the tri-layer window from left to right and top to bottom on a raw IR image, calculate each pixel's multiscale TLLCM value according to the following steps.

1) For Core Layer: The theory of the matched filter tells us the best filter for enhancing a signal should have the same shape as the signal [25]. However, current algorithms do not fully consider the target shape and may be easily disturbed by noises. For example, the LCM just uses the maximal value of the central cell, and it is sensitive to PNHB; the improved LCM (ILCM) [6] adopts the mean value of the central cell to suppress PNHB, but the small target may be smoothed too; the novel LCM (NLCM) [15] and the relative LCM (RLCM) [17] only consider K maximal pixels of the central cell to avoid smoothing target; however, they are sensitive to scattered noises, see Fig. 3 (left).

In this letter, considering that a true target usually has a compact 2-D Gaussian-like shape, a Gaussian filter is applied on the core layer, and the enhanced result of the core layer will be

$$I_{\text{core}}(x, y) = \sum_{l=-1}^{1} \sum_{k=-1}^{1} GS(l, k) I(x + l, y + k) \tag{1}$$

where (x, y) is the coordinate of a pixel, I is the raw image, and I_{core} is the enhanced result, which will be used as a key parameter for local contrast calculation next. GS is the Gaussian template, and in this letter, a commonly used normalized template is selected, GS = [1/16, 1/8, 1/16; 1/8, 1/4, 1/8; 1/16, 1/8, 1/16].

Fig. 3 (right) shows that compared to some existing algorithms, the Gaussian filter used in the proposed algorithm can suppress scattered noises better.

2) For Surrounding Layer: To suppress complex background as far as possible, for each cell of the surrounding layer, calculate the average value of the K maximal pixels as another key parameter, that is,

$$I_{\text{surr}}(i) = \frac{1}{K} \sum_{j=1}^{K} G_i^j, \quad i = 1, 2, \ldots, 8 \tag{2}$$

where G_i^j is the jth maximal gray value of cell(i), and K is the number of pixels considered and is set to 9, which is equal to the pixels of the core layer to get an accurate local contrast next.

3) Multiscale TLLCM Between Core and Surroundings: The local contrast information will be calculated between the enhanced core and the surroundings. There have been many

definitions of local contrast by now, which can be roughly divided into the ratio-form and the difference-form [17]. The ratio-form local contrast can enhance true target, and the difference-form local contrast can eliminate a high brightness background. In this letter, both the ratio and difference operations are used to calculate the local contrast information, and for each pixel, its single-scale TLLCM is defined as follows:

$$\mathrm{TLLCM} = \min\left(\frac{I_{\mathrm{core}}}{I_{\mathrm{surr}}(i)} I_{\mathrm{core}} - I_{\mathrm{core}}\right), \quad i = 1, 2, \ldots, 8 \tag{3}$$

where the min operation between eight directions is used to suppress background edges.

Considering that the size of the target is usually unknown in practice, multiscale detection will be needed, i.e., set the size of the reserve layer to different scales, for each scale, calculate the single-scale TLLCM according to (1)–(3), then use a max pooling between different scales

$$\mathrm{TLLCM} = \max(0, \mathrm{TLLCM}_p), \quad p = 1, 2, \ldots, L \tag{4}$$

where p means the pth scale and L is the total number of scales. Note that a nonnegative constraint is used to suppress clutters further since a true target is usually brighter than its neighbors.

C. Threshold Operation

For each pixel of the raw image, calculate the multiscale TLLCM and form the results as a new matrix named saliency map (SM). It is necessary to discuss the different situations when a pixel (x, y) is a true target center, pure background, background edge, broken cloud, or PNHB.

1) If (x, y) is true target center, then its I_{core} will be large, I_{surr} will be small, and so its TLLCM will be larger than 0.
2) If (x, y) is pure background (including high brightness background), since the background is usually continuously distributed over a wide area, its I_{core} will be close to I_{surr}, and there will be TLLCM ≈ 0.
3) If (x, y) is background edge, since a min operation is used in (3), there will be TLLCM ≈ 0, too.
4) If (x, y) is broken cloud, since broken cloud is usually local salient, its I_{core} may be larger than I_{surr}, and so its TLLCM value will be larger than 0. However, a broken cloud usually has a smaller gray value than true target [5], so its TLLCM will be smaller than a true target, and it will not disturb the target detection.
5) If (x, y) is a PNHB whose gray value is similar to that of the true target, since PNHB usually emerges as a single pixel, it is not Gaussian-like, so its I_{core} and TLLCM will be smaller than a true target, and it will not disturb the detection, too.

From the discussions above, it can be seen that in SM, the true target will be the most salient, and other interferences will be suppressed. Thus, a simple threshold operation [26] will be used to extract the true target, and the threshold is defined as

$$\mathrm{Th} = \lambda \max_{\mathrm{SM}} + (1 - \lambda)\mathrm{mean}_{\mathrm{SM}} \tag{5}$$

where $\max_{\mathrm{SM}}$ and $\mathrm{mean}_{\mathrm{SM}}$ are the maximum and average of SM, respectively. λ is a given factor between 0 and 1, if it is set to 0, the threshold will be equal to $\mathrm{mean}_{\mathrm{SM}}$, and if it is set to 1, the threshold will be equal to $\max_{\mathrm{SM}}$. Our experiments show that 0.7–0.9 will be proper for single target detection since the target is very salient and the clutters are well suppressed.

TABLE I
DETAILS OF THE SEVEN SEQUENCES

	Frames	Size	Target number	Target size	Target type
Seq. 1	200	320×240	1	4×3 to 7×5	Plane target
Seq. 2	70	256×200	1	4×5 to 4×10	Plane target
Seq. 3	200	320×256	1	3×5	Plane target
Seq. 4	200	320×256	1	3×3	Plane target
Seq. 5	100	256×256	1	3×5	Truck target
Seq. 6	200	280×228	2	5×5	Ship target
Seq. 7	100	256×256	4	5×5 to 7×5	Ship target

III. Experimental Results

To illustrate the effectiveness of the proposed algorithm, seven real IR sequences that contain different sizes and different types of small targets are used for experiments. Table I gives the details of the seven sequences.

Fig. 4 shows the detection results using the proposed algorithm step by step. The first column is the raw image samples, and it can be seen that the targets are small and dim and the backgrounds are complex. The second to the fourth columns are the single-scale TLLCM calculation results, three scales are used here, in which s is set to 5, 7, and 9, respectively. It can be seen that a larger target will be more salient in the larger scale, and vice versa. The fifth column is the final multiscale TLLCM results (normalized). It can be seen that the targets will be the most salient in SM, while other interferences are well suppressed. The last column is the detection results after threshold operation, all the true targets are output successfully, and no false alarm occurs, which proves that the proposed algorithm can effectively deal with different types and different sizes of targets under complex background.

Then, some existing local contrast algorithms are chosen for comparisons, including DoG [8], variance difference (VAR-DIFF) [12], ILCM [6], NLCM [15], multiscale patch-based contrast measure (MPCM) [16], RLCM [17], weighted local difference measure (WLDM) [19], and multidirectional 2-D least mean-square and ratio-difference joint LCM (MDTDLMS-RDLCM) [23]. DoG is a basic local contrast method without using directional information. VAR-DIFF is a tri-layer method without using directional information. ILCM and NLCM are both directional methods. MPCM and RLCM are both multiscale directional methods. WLDM and MDTDLMS-RDLCM are both methods combined with other algorithms. The parameter settings of all the compared methods are consistent with the authors' suggestions.

First, for each sample of the seven sequences, Tables II and III give the SCR gain (SCRG, which can be used to describe the target enhancement ability) and background suppress factor (BSF, which can be used to describe the background suppression ability) of each algorithm, here the SCRG is defined as the ratio between the SCR of SM and the SCR of raw image and BSF is defined as the ratio between the standard deviation of raw image and the standard deviation of SM.

In Tables II and III, it can be seen that the proposed algorithm can achieve the best SCRG for six of the eleven targets,

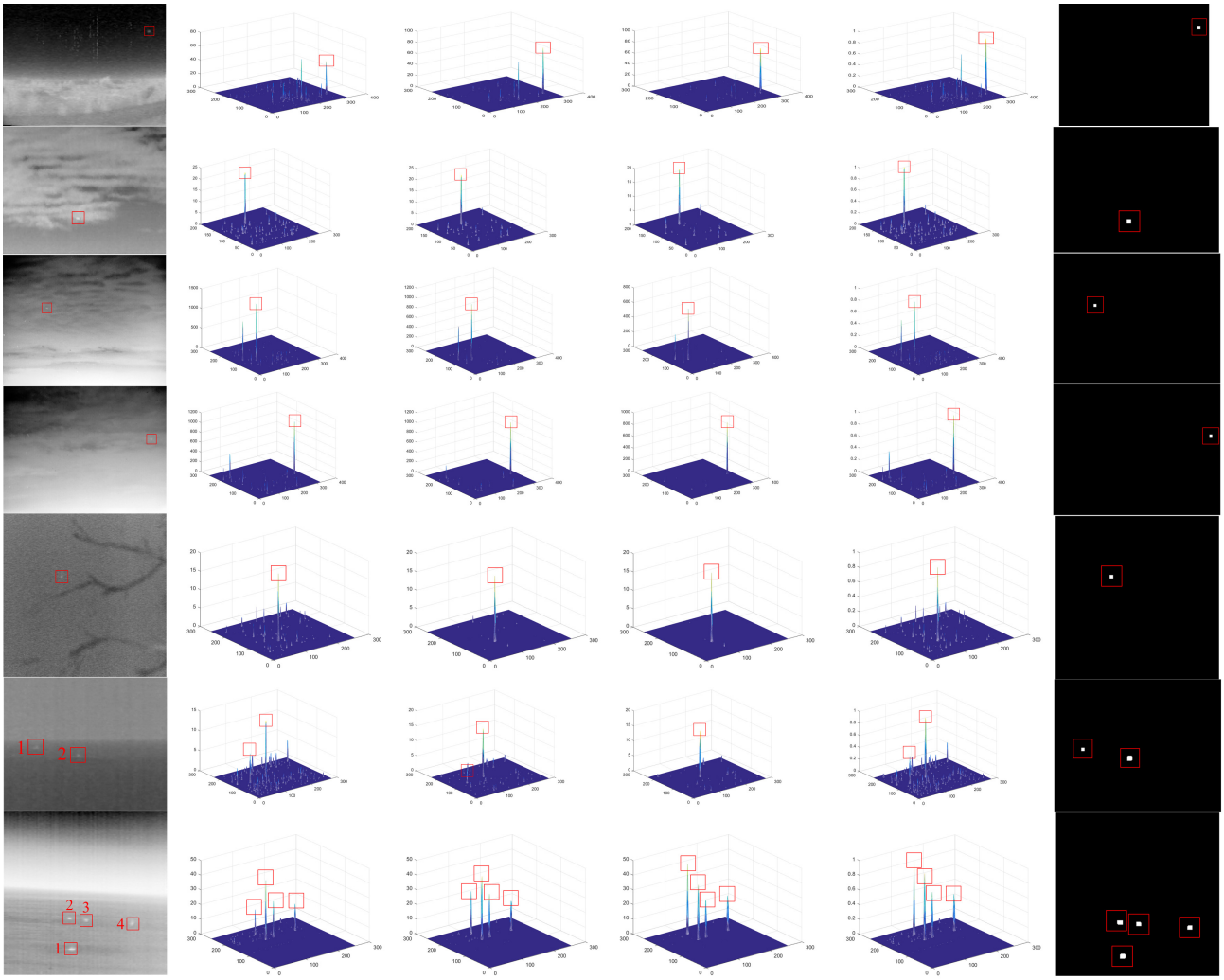

Fig. 4. From top to bottom: the detection results of Seq. 1–Seq. 7 using the proposed algorithm. (a) Raw IR image. (b)–(d) Single-scale TLLCM result when s is set to 5, 7, and 9, respectively. (e) Final multiscale TLLCM result (normalized). (f) Detection result after threshold operation.

TABLE II
SCRG OF DIFFERENT ALGORITHMS

Seq	Target	DoG	VAR-DIFF	ILCM	NLCM	MPCM	RLCM	WLDM	MDTDLMS-RDLCM	Proposed
1	1	6.2885	92.1675	7.2875	10.1899	7.6446	15.7705	18.5764	51.2914	**102.5329**
2	1	1.9132	**44.2458**	6.0963	5.6193	2.9264	2.5565	7.8443	12.6830	28.1468
3	1	8.3011	24.4902	13.0714	18.8765	2.8125	11.8627	46.2286	48.9359	**171.0698**
4	1	9.3889	198.1542	17.0028	30.2450	9.5588	17.6710	45.1927	101.2353	**227.9375**
5	1	1.5289	23.2185	2.5832	4.4538	2.9411	2.5795	4.2662	8.7117	**30.2972**
6	1	14.9848	**73.8877**	13.6793	14.2903	10.8889	5.4331	46.9801	37.9182	42.6979
	2	9.1796	**157.7197**	8.4822	12.0151	9.0312	7.2304	24.8754	34.3315	59.1686
7	1	8.4327	**48.5450**	4.4035	0.3047	8.3807	8.1419	38.6412	35.3682	39.7094
	2	6.0860	22.5104	14.0724	7.6629	6.4653	7.0714	34.1497	44.1577	**44.3881**
	3	5.9508	6.8973	3.5529	2.8184	8.9205	6.5915	19.3874	**43.4040**	43.2326
	4	5.3314	4.4662	3.4226	0.0654	6.9744	6.5919	18.1551	37.2507	**37.3533**

and for the other five targets, the SCRG of the proposed algorithm is also very large. In addition, the proposed algorithm can achieve the best BSF for all seven sequences. It is because the proposed algorithm can enhance true target purposefully according to its shape, besides, the ratio-difference joint local contrast in (3) and the nonnegative constraint in (4) can further improve the detection performance.

Then, the receiver-operating-characteristic (ROC) curves of different algorithms are shown in Fig. 5, here the true positive rate (TPR) is defined as the ratio between the number of detected true targets and the total number of true targets, and the false positive rate (FPR) is defined as the ratio between the number of detected false targets and the total number of pixels in the whole image. It can be seen that the proposed algorithm can achieve a good detection performance in most cases.

Finally, we will discuss the computational complexity. Suppose the core size is $c \times c$ and the cell size is $R \times R$ ($c < R$), for core layer, there will be c^2 multiplications and c^2 additions; for surrounding layer, there will be $R^2 \log R^2$ sorting operations, K (equal to c^2) additions, and 1 multiplication

TABLE III
BSF OF DIFFERENT ALGORITHMS

Seq	DoG	VAR-DIFF	ILCM	NLCM	MPCM	RLCM	WLDM	MDTDLMS-RDLCM	Proposed
1	2.1241	0.0028	33.9468	1.4121	0.5767	6.1397	681.6723	3.4236E3	**4.3918E3**
2	0.7403	0.0119	17.4796	1.0426	0.3002	2.7740	112.1502	660.7865	**1.4532E3**
3	3.2310	2.8464E-10	49.5869	0.0361	0.0202	11.1200	15.1272	1.3470E5	**4.6379E5**
4	7.1437	3.8129E-9	94.5928	0.1103	0.0299	15.3791	39.7668	1.8704E5	**4.1668E5**
5	0.7329	0.0030	10.4656	0.8334	0.5660	2.8416	81.8911	316.0840	**1.0835E3**
6	3.9246	0.0539	59.0583	10.9018	1.4717	6.1755	1.6762E3	992.0782	**1.6974E3**
7	2.1606	1.6158E-4	29.8661	0.6584	0.7421	5.2646	536.9486	2.3261E3	**2.5676E3**

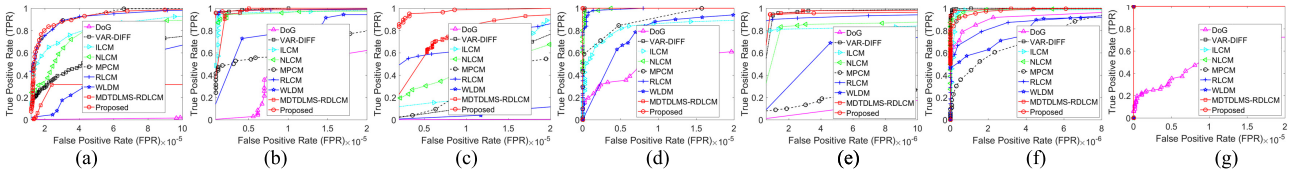

Fig. 5. ROC curves of different algorithms for (a) Seq. 1, (b) Seq. 2, (c) Seq. 3, (d) Seq. 4, (e) Seq. 5, (f) Seq. 6, and (g) Seq. 7.

for each cell, totally there will be $8(R^2\log R^2+ c^2+ 1)$ operations; for single-scale TLLCM calculation, there will be 2 multiplications and 1 addition. Thus, for an $M \times N$ image using L scales, $L \times [2c^2+ 8(R^2\log R^2 + c^2+ 1) + 3] \times MN$ operations will be needed, and the computational complexity of the proposed algorithm is $O(LR^2\log R^2MN)$, which is the same as RLCM.

IV. CONCLUSION

In this letter, a new framework for IR small target detection is proposed, in which the target will be enhanced before local contrast calculation. By adopting the idea of the matched filter, a Gaussian filtering operation will be performed on the core layer to enhance true target purposefully according to the target shape. Experimental results show that the proposed algorithm can achieve a good detection performance for different types and different sizes of IR small targets.

REFERENCES

[1] Y. Chen, B. Song, D. Wang, and L. Guo, "An effective infrared small target detection method based on the human visual attention," *Infr. Phys. Technol.*, vol. 95, pp. 128–135, Dec. 2018.

[2] P.-Y. Lv, S.-L. Sun, C.-Q. Lin, and G.-R. Liu, "Space moving target detection and tracking method in complex background," *Infr. Phys. Technol.*, vol. 91, pp. 107–118, Jun. 2018.

[3] X. Bai and Y. Bi, "Derivative entropy-based contrast measure for infrared small-target detection," *IEEE Trans. Geosci. Remote Sens.*, vol. 56, no. 4, pp. 2452–2466, Apr. 2018.

[4] K. Liang, Y. Ma, Y. Xie, B. Zhou, and R. Wang, "A new adaptive contrast enhancement algorithm for infrared images based on double plateaus histogram equalization," *Infr. Phys. Technol.*, vol. 55, no. 4, pp. 309–315, Jul. 2012.

[5] X. Yang, Y. Zhou, D. Zhou, R. Yang, and Y. Hu, "A new infrared small and dim target detection algorithm based on multi-directional composite window," *Infr. Phys. Technol.*, vol. 71, pp. 402–407, Jul. 2015.

[6] J. Han, Y. Ma, B. Zhou, F. Fan, K. Liang, and Y. Fang, "A robust infrared small target detection algorithm based on human visual system," *IEEE Geosci. Remote Sens. Lett.*, vol. 11, no. 12, pp. 2168–2172, Dec. 2014.

[7] S. Kim, Y. Yang, J. Lee, and Y. Park, "Small target detection utilizing robust methods of the human visual system for IRST," *J. Infr., Millim., THz Waves*, vol. 30, no. 9, pp. 994–1011, Sep. 2009.

[8] X. Wang, G. Lv, and L. Xu, "Infrared dim target detection based on visual attention," *Infr. Phys. Technol.*, vol. 55, no. 6, pp. 513–521, Nov. 2012.

[9] X. Shao, H. Fan, G. Lu, and J. Xu, "An improved infrared dim and small target detection algorithm based on the contrast mechanism of human visual system," *Infr. Phys. Technol.*, vol. 55, no. 5, pp. 403–408, Sep. 2012.

[10] J. Han, Y. Ma, J. Huang, X. Mei, and J. Ma, "An infrared small target detecting algorithm based on human visual system," *IEEE Geosci. Remote Sens. Lett.*, vol. 13, no. 3, pp. 452–456, Mar. 2016.

[11] X. Wang, Z. Peng, P. Zhang, and Y. He, "Infrared small target detection via nonnegativity-constrained variational mode decomposition," *IEEE Geosci. Remote Sens. Lett.*, vol. 14, no. 10, pp. 1700–1704, Oct. 2017.

[12] M. Nasiri and S. Chehresa, "Infrared small target enhancement based on variance difference," *Infr. Phys. Technol.*, vol. 82, pp. 107–119, May 2017.

[13] J. Han, Y. Yu, K. Liang, and H. Zhang, "Infrared small-target detection under complex background based on subblock-level ratio-difference joint local contrast measure," *Opt. Eng.*, vol. 57, no. 10, Oct. 2018, Art. no. 103105.

[14] C. L. P. Chen, H. Li, Y. Wei, T. Xia, and Y. Y. Tang, "A local contrast method for small infrared target detection," *IEEE Trans. Geosci. Remote Sens.*, vol. 52, no. 1, pp. 574–581, Jan. 2014.

[15] Y. Qin and B. Li, "Effective infrared small target detection utilizing a novel local contrast method," *IEEE Geosci. Remote Sens. Lett.*, vol. 13, no. 12, pp. 1890–1894, Dec. 2016.

[16] Y. Wei, X. You, and H. Li, "Multiscale patch-based contrast measure for small infrared target detection," *Pattern Recognit.*, vol. 58, pp. 216–226, Oct. 2016.

[17] J. Han, K. Liang, B. Zhou, X. Zhu, J. Zhao, and L. Zhao, "Infrared small target detection utilizing the multiscale relative local contrast measure," *IEEE Geosci. Remote Sens. Lett.*, vol. 15, no. 4, pp. 612–616, Apr. 2018.

[18] J. Nie, S. Qu, Y. Wei, L. Zhang, and L. Deng, "An infrared small target detection method based on multiscale local homogeneity measure," *Infr. Phys. Technol.*, vol. 90, pp. 186–194, May 2018.

[19] H. Deng, X. Sun, M. Liu, C. Ye, and X. Zhou, "Entropy-based window selection for detecting dim and small infrared targets," *Pattern Recognit.*, vol. 61, pp. 66–77, Jan. 2017.

[20] Z. Cui, J. Yang, S. Jiang, J. Li, L. Lin, and Y. Gu, "An infrared-small-target detection method in compressed sensing domain based on local segment contrast measure," *Infr. Phys. Technol.*, vol. 93, pp. 41–52, Sep. 2018.

[21] S. Moradi, P. Moallem, and M. F. Sabahi, "A false-alarm aware methodology to develop robust and efficient multi-scale infrared small target detection algorithm," *Infr. Phys. Technol.*, vol. 89, pp. 387–397, Mar. 2018.

[22] C. Xia, X. Li, and L. Zhao, "Infrared small target detection via modified random walks," *Remote Sens.*, vol. 10, no. 12, p. 2004, 2018.

[23] J. Han, S. Liu, G. Qin, Q. Zhao, H. Zhang, and N. Li, "A local contrast method combined with adaptive background estimation for infrared small target detection," *IEEE Geosci. Remote Sens. Lett.*, vol. 16, no. 9, pp. 1442–1446, Sep. 2019.

[24] Y. Qin, L. Bruzzone, C. Gao, and B. Li, "Infrared small target detection based on facet kernel and random walker," *IEEE Trans. Geosci. Remote Sens.*, vol. 57, no. 9, pp. 7104–7118, Sep. 2019.

[25] S. Moradi, P. Moallem, and M. F. Sabahi, "Scale-space point spread function based framework to boost infrared target detection algorithms," *Infr. Phys. Technol.*, vol. 77, pp. 27–34, Jul. 2016.

[26] H. Fu, Y. Long, R. Zhu, and W. An, "Infrared small target detection based on multiscale center-surround contrast measure," *Proc. SPIE*, vol. 10615, pp. 106150I-1–106150I-08, Apr. 2018.